

Short Communication

## Corrosion Behavior and Magnetic Property Degradation of FeCrNiTi Soft Magnetic Materials in NaCl-containing environments

Zhongsheng Li<sup>1</sup>, Xianlong Cao<sup>2,\*</sup>, Dalong Cong<sup>1</sup>, Kaiqiang Song<sup>1</sup>, Xiaowei Liu<sup>2</sup>, Jiling Dong<sup>2</sup>, Zhiyong Zhou<sup>2</sup>

<sup>1</sup> Southwest Institute of Technology and Engineering, Chongqing 400039, China

<sup>2</sup> Chongqing University of Science and Technology, Chongqing 401331, China

\*E-mail: [xianlong@cqust.edu.cn](mailto:xianlong@cqust.edu.cn)

Received: 3 May 2022 / Accepted: 5 July 2022 / Published: 7 August 2022

---

The corrosion behavior of FeCrNiTi soft magnetic materials has been studied in different concentrations of NaCl solution over different immersion times using electrochemical methods. Changes in the magnetic properties of FeCrNiTi materials after salt spray testing were evaluated. Results showed that the open circuit potential became more negative and the corrosion current density increased with increasing NaCl solution concentration. Nyquist plots demonstrated similar shapes and only displayed one capacitive loop over the frequency range, the radius of the capacitive loop gradually decreased with the NaCl concentration and immersion time, and the corrosion process was controlled by a charge transfer mechanism. Corrosion occurred preferentially in the surface area with low Ti content, and the area covered with a Ti-rich surface film had a relatively strong corrosion resistance. Rupturing of the protective oxide film was shown to occur more easily at lower critical potentials at higher NaCl solution concentrations. The magnetic properties of FeCrNiTi were shown to be degraded by corrosion due to the formation of corrosion products, the precipitation of Fe elements from the matrix, and the internal stress induced by corrosion pits.

---

**Keywords:** Soft magnetic materials, Corrosion behavior, Electrochemical corrosion measurement, Salt spray test, Magnetic property degradation

### 1. INTRODUCTION

Soft magnetic alloys have been widely used due to their high maximum magnetic permeability and initial magnetic permeability, low coercivity, high saturation magnetization, and low remanent magnetization [1,2]. With the rapid development of automation technology, iron-based soft magnetic alloys, as one of the most important categories of soft magnetic alloys, have become very important functional materials in the fields of radio, motors, communications, home appliances and computers [2].

However, the iron-based soft magnetic alloy often serves in the marine environment containing chlorides or a humid industrial environment, where it is susceptible to atmospheric corrosion and local corrosion [3,4]. The corrosion may affect its magnetic properties and service life and may cause serious economic losses [5].

So far, much attention has been paid to the alloys. However, there are few works in the literature associated with their corrosion behavior in aggressive environments and the effects of corrosion on the magnetic properties [6]. Hayashi *et al.* [7] pointed out that FeCo-based alloys showed good atmospheric corrosion-resistant performance and preferable magnetic properties. May *et al.* [8] indicated that a large decrease (about 20%) in the magnetic properties of FeCo-based alloys can be caused by corrosion. Mariano *et al.* [9] noted that the saturation magnetic flux density of FeCuNbSiB alloys exhibited a slight decrease, likely caused by the corrosion process of the alloys. Ouadah *et al.* [10] found that when the corrosion was presented in the magnetic circuits of an induction machine, the hysteresis loss increased, which consequentially reduced the machine efficiency. Peng *et al.* [11] reported that the corrosion resistance of amorphous FeZrNbBCu alloys showed obvious decreases after partial crystallization and protective oxide layers could be observed on the surface of this alloy after corrosion, which resulted in poor soft magnetic properties, higher threshold field, and higher relaxation frequency. Szewieczek *et al.* [12] found that the corrosion occurring on the surface of the FeSiNbCu alloy can lead to a reduction in local defects caused by impurities and can also degrade the magnetic properties of this alloy. Sitek *et al.* [13] studied the corrosion and the effects of corrosion on the magnetic properties of amorphous and nanocrystalline Finemet and Nanoperm. They indicated that the nanocrystalline sample was more corrosion resistant than the amorphous version, and the surface saturation magnetization of the former after corrosion did not change significantly, but the surface saturation magnetization of the latter obviously decreased [13].

The above-mentioned results indicate that the magnetic properties can be affected by the surface corrosion of soft magnetic alloys because these properties can be influenced by the surface quality [11,14]. Furthermore, the influence of corrosion on the magnetic properties of these materials can be usually stated by the presence of non-conductor and/or non-magnetic oxides on the corroded surfaces. However, the results mainly stem from the amorphous alloys and there is a disagreement between the results from different researchers.

Therefore, this paper focuses on crystalline soft magnetic alloys and investigates the corrosion behaviors and magnetic property degradation of FeCrNiTi soft magnetic alloy specimens in NaCl-containing environments. Electrochemical corrosion measurements and neutral salt spray tests were carried out, and corrosion morphology observations, corrosion products analysis, and magnetic properties measurements were performed.

## 2. EXPERIMENTAL

### 2.1. Materials and solutions

The FeCrNiTi soft magnetic materials used in this work were purchased from Central Iron & Steel Research Institute (China). The chemical compositions of the soft magnetic materials are given in

Table 1. All FeCrNiTi specimens were cut into circular shapes and then welded with copper wire with an insulated protective layer. The FeCrNiTi specimens were sealed with a cured epoxy resin, and only one working surface with an area of around 2 cm<sup>2</sup> remained. The left surface was ultrasonically washed with ethanol for 10 min and then deionized water for 10 min, and finally dried with compressed air for use.

The experimental solutions included 40, 60 and 70 g/L NaCl prepared with analytical reagent grade NaCl and deionized water.

**Table 1.** Chemical composition of FeCrNiTi soft magnetic materials (wt.%)

<i>C</i>	<i>Si</i>	<i>Mn</i>	<i>P</i>	<i>S</i>	<i>Cr</i>	<i>Ni</i>	<i>Ti</i>	<i>Fe</i>
0.012	0.13	0.47	0.0052	0.0036	18.06	0.62	0.61	Bal.

## 2.2. Electrochemical measurements

Electrochemical tests were performed via a traditional three-electrode configuration connected to an electrochemical measurement system (CHI660E, Shanghai CHI, China). The three-electrode configuration consisted of the working electrode (WE), counter electrode (CE), and reference electrode (RE), which corresponded to the FeCrNiTi specimen sealed with epoxy, a platinum net electrode, and an Ag/AgCl/saturated KCl electrode, respectively. The electrochemical tests of the FeCrNiTi specimens included open circuit potential (OCP) testing, potentiodynamic polarization testing, and electrochemical impedance spectroscopy (EIS). All tests were carried out after immersion in 40, 60, and 70 g/L NaCl solution at 35 °C over different durations (72, 120, 168, 240 h). The solutions were heated in a water bath with automatic temperature control. The open circuit potentials of the specimens were recorded during the initial 100 s after immersion in NaCl solution. For EIS testing, the EIS frequencies were scanned from 0.01 Hz to 100 kHz, and the AC signal amplitude potential was set to 10 mV (vs. OCP). The potentiodynamic polarization curves were scanned from -0.4 V to +1.5 V (vs. OCP) and the scanning rate was set to 1 mV/s.

## 2.3. Neutral salt spray test

Neutral salt spray (NSS) testing of the FeCrNiTi specimens were conducted in a salt spray test chamber (FQY025, Shanghai Laboratory Instrument Works Co., Ltd, China) at 35 °C according to ASTM B117 Standard Salt Spray testing. The spray solution was 5 wt.% NaCl solution, and its pH was adjusted to 6.5–7.2. The sedimentation rate of salt spray should be controlled between 1–2 mL/80 cm<sup>2</sup>·h. The circular FeCrNiTi specimens were placed in a test chamber and directly exposed to salt spray. The specimens were removed from the chamber after different salt spray corrosion times (24, 48, 72, and 200 h) to evaluate the magnetic properties. In addition, the surface morphology and elemental composition were examined by scanning electron microscopy (SEM) and energy dispersive spectroscopy (EDS) analyzer. Before all examinations, the specimens were gently cleaned with running

water and then alcohol so as to clear away salt deposits from the surface, followed by quick drying with cold compressed air.

#### 2.4. Characterization of corrosion products

After immersion in NaCl solution at 35 °C for 240 h, X-ray diffraction patterns of corrosion products of the FeCrNiTi specimen were obtained using an X-ray diffractometer (DX-2700, Shandong Fangyuan, China) operating at 30 kV and 20 mA. The XRD data were recorded within a 2 $\theta$  range of 5–90 ° at a scanning rate of 0.04° per step using Cu K $\alpha$  radiation.

After salt spray testing for 200 h, the surface morphology and elemental composition of the FeCrNiTi specimens were studied by a SEM (S-3700N, Hitachi, Japan) equipped with an EDX analyzer.

#### 2.5. Characterization of magnetic properties

The magnetic properties of the FeCrNiTi specimens after salt spray testing for varying durations were evaluated by a soft magnet test system (MATS-2010S, China) with a maximum applied magnetic field of 5 kOe at room temperature. The magnetic parameters extracted from the hysteresis loops of the soft magnetic alloy FeCrNiTi were the initial magnetic permeability ( $\mu_i$ ), maximum magnetic permeability ( $\mu_m$ ), saturation magnetization ( $B_s$ ), coercivity ( $H_c$ ), remanent magnetization ( $B_r$ ), and hysteresis loss ( $P_u$ ).

### 3. RESULTS AND DISCUSSION

#### 3.1. Electrochemical corrosion behaviors after immersion tests

##### 3.1.1 Open circuit potential

Figure 1 shows the evolution of open circuit potential of FeCrNiTi soft magnetic alloy specimens after 240 h immersion in 40, 60, and 70 g/L NaCl aggressive solution at 35 °C.

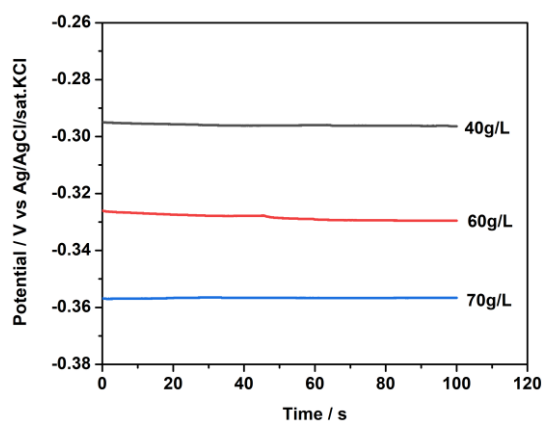


**Figure 1.** Open circuit potentials of FeCrNiTi soft magnetic alloy specimens after 240 h immersion in 40, 60, and 70 g/L NaCl aggressive solution at 35 °C

After immersion for 240 h, the OCP of each FeCrNiTi specimen remained stable, which shows that the specimens were in a steady corrosive state. At this time, the overall corrosion possibly dominated the whole corrosion reaction process or no new localized corrosion occurred by chloride ions, which indicates no abrupt potential caused by localized corrosion. The OCP values of the specimens in 40, 60, and 70 g/L NaCl solution were around  $-0.296$  V,  $0.329$  V and  $-0.356$  V, respectively. From the perspective of corrosion thermodynamics, the more positive the open circuit potential is, the less likely the metal is to corrode. [15]. It can be noticed that the OCP of the specimens gradually became more negative with increasing NaCl solution concentration, which means that the increase in NaCl solution concentration can increase the possibility of corrosion of FeCrNiTi soft magnetic alloys [15].

### 3.1.2 Potentiodynamic polarization curves

Potentiodynamic polarization curves of FeCrNiTi soft magnetic alloy specimens after 240 h immersion in 40, 60, and 70 g/L NaCl aggressive solution at  $35$  °C are illustrated in Fig. 2. Table 2 summarizes the fitting results of the potentiodynamic polarization curves of FeCrNiTi specimens, where  $i_{\text{corr}}$  is the corrosion current density ( $\mu\text{A}/\text{cm}^2$ ),  $E_{\text{corr}}$  the corrosion potential (V), and  $b_a$  the anodic Tafel slope (mV/dec).

Generally speaking, it is common knowledge that a higher  $E_{\text{corr}}$  and lower  $i_{\text{corr}}$  correlates to better corrosion resistance [16]. With increasing NaCl solution concentration, the corrosion potential  $E_{\text{corr}}$  gradually became more negative and the anodic Tafel slope  $b_a$  decreased, which indicates that the corrosion of the FeCrNiTi specimens was more likely to occur when the concentration of NaCl solution increased. Moreover, the corrosion current density  $i_{\text{corr}}$  increased with the concentration of NaCl solution, although the changes in corrosion current density were relatively insignificant.

In addition, it can be observed that all the cathodic branches showed almost the same shape, as well as the anodic branches. The anodic polarization curves of the FeCrNiTi specimen have a slightly passive platform [16] and the anodic Tafel region is still clear. For the cathodic reaction in neutral NaCl solutions open to the air, oxygen is reduced to hydroxyl ions ( $\text{O}_2 + 2\text{H}_2\text{O} + 4\text{e}^- \rightarrow 4\text{OH}^-$ ). The anodic reaction is the oxidation of Fe to ferrous ions ( $\text{Fe} \rightarrow \text{Fe}^{2+} + 2\text{e}^-$ ) resulting in anodic dissolution [17,18]. When the anodic branches were polarized to potentials of  $0.506$  V,  $0.321$  V, and  $0.301$  V in 40, 60, and 70 g/L NaCl aggressive solution, respectively, the corrosion current density suddenly increased, which may be due to the rupture of the protective oxide film or corrosion product film on the surface of the FeCrNiTi specimens. The potentials are the critical polarization potential causing surface film ruptures. It is known that the critical potentials of the specimens will be more negative and the changes in corrosion current density were more obvious at higher NaCl solution concentrations.

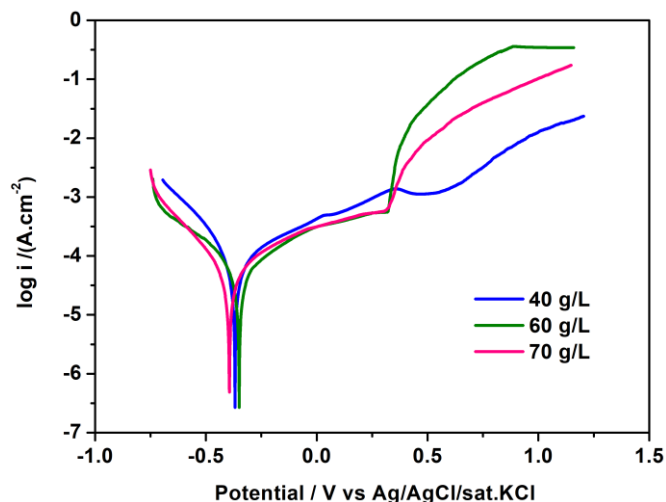


**Figure 2.** Potentiodynamic polarization curves of FeCrNiTi soft magnetic alloy specimens in 40, 60, and 70 g/L NaCl aggressive solution after immersion for 240 h at 35 °C

**Table 2.** Electrochemical parameters for potentiodynamic polarization curves of FeCrNiTi soft magnetic alloy specimens after 240 h immersion in 40, 60, and 70 g/L NaCl aggressive solution at 35 °C

$C_{\text{NaCl}}$ (g/L)	$E_{\text{corr}}$ (V)	$E_b$ (V)	$i_{\text{corr}}$ ( $\mu\text{A}\cdot\text{cm}^{-2}$ )	$b_a$ (mV/dec)
40	-0.369	0.506	33.5	301
60	-0.350	0.321	46.2	212
70	-0.394	0.301	55.7	203

### 3.1.3 Electrochemical impedance spectroscopy

The EIS Nyquist plots of the corrosion of FeCrNiTi soft magnetic alloy specimens after immersion in 40, 60, and 70 g/L NaCl aggressive solution at 35 °C over varying durations are illustrated in Fig. 3a-c.

All Nyquist plots of the corrosion of FeCrNiTi have similar shapes and only one displayed a semicircular capacitive loop over the entire frequency range for different NaCl solutions and different immersion times. A Nyquist plot with a single semicircular capacitive loop means that the corrosion electrochemical reaction is primarily governed by the charge transfer process at the interface between the solution and metal [19]. Furthermore, it is worth noting that all the semicircles were depressed, which represents a certain dispersion effect. This effect may be due to heterogeneity of the tested surface and the charge distribution in the EIS tests [14], such as the uneven phenomenon of the electrode surface caused by corrosion or the formation of a corrosion product film. Thus, the electric double layer of the FeCrNiTi electrode in the NaCl solution deviated from the ideal capacitance state.

Here, the most common equivalent electrical circuit used for a metal corrosion model in aqueous electrolyte was adopted, as shown in Fig. 3d. The equivalent circuit consisted of a solution resistance  $R_s$ , metal charge transfer resistance  $R_{ct}$ , and capacitance of constant phase element  $CPE$  after fitting and simulation. The fitted EIS results of the FeCrNiTi soft magnetic alloy specimens obtained using the proposed equivalent electrical circuit are listed in Table 3.

Generally, a larger capacitive loop indicates good corrosion resistance [20]. According to Fig. 3 and Table 3, it is observed that the radius of the capacitive loop and  $R_{ct}$  gradually decreased with increasing NaCl concentration. In addition, with prolonged immersion time, the radius of the capacitive loop and  $R_{ct}$  also gradually decreased. These results mean that the corrosion resistance of the FeCrNiTi soft magnetic alloy specimens gradually decreased with increasing NaCl solution concentration and immersion time. This coincides with the results from the potentiodynamic polarization testing.

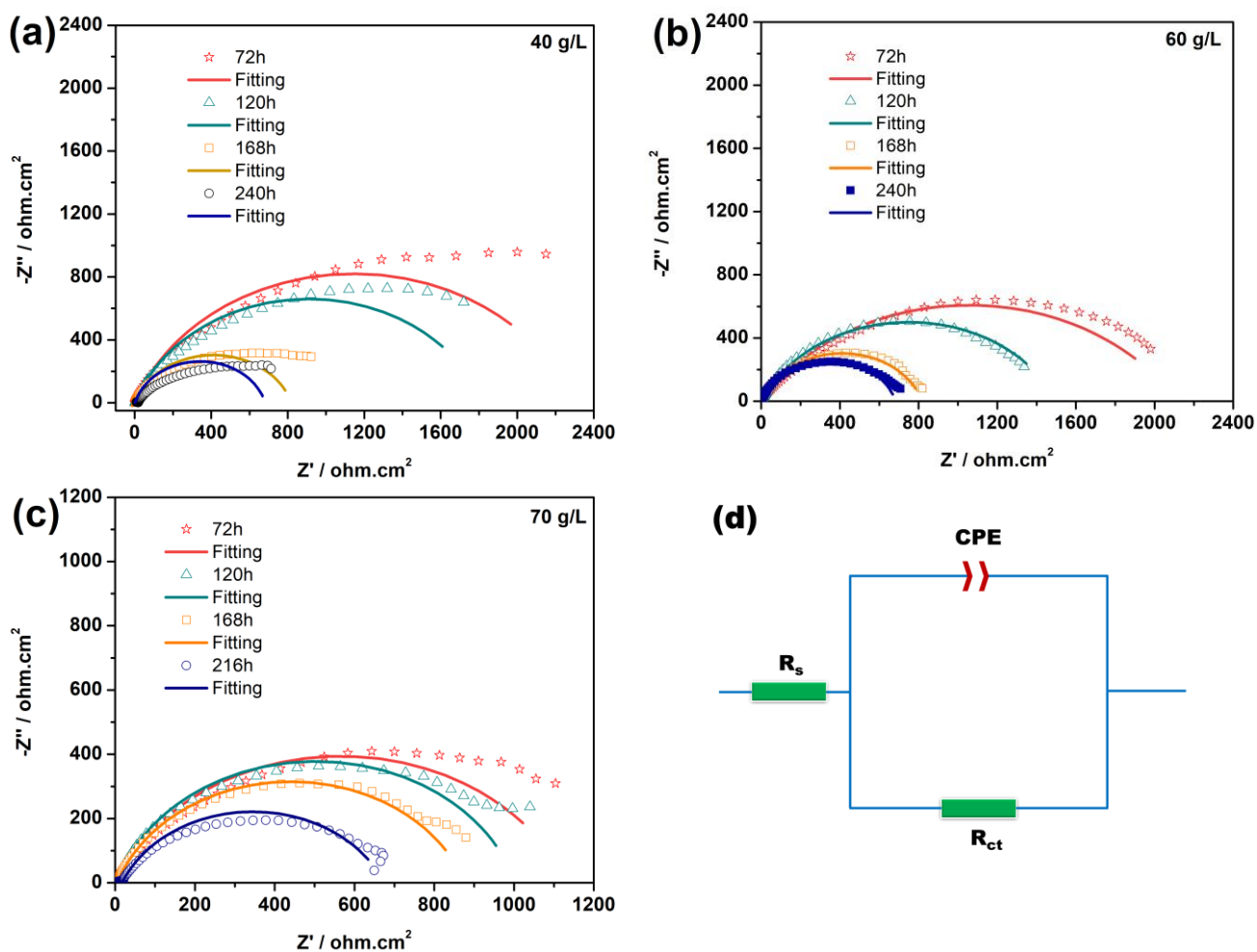


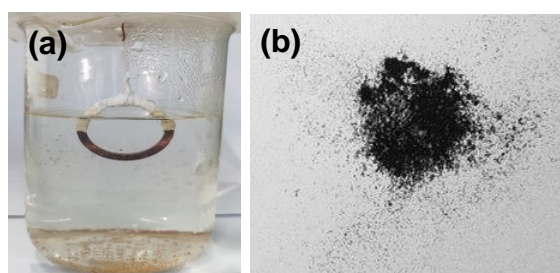
**Figure 3.** EIS plots of the corrosion of FeCrNiTi soft magnetic alloy specimens after immersion in 40 (a), 60 (b), and 70 g/L (c) NaCl aggressive solution at 35 °C for different hours and the corresponding equivalent circuit model (d)

**Table 3.** EIS fitting results for the corrosion of FeCrNiTi soft magnetic alloy specimens in 40, 60, and 70 g/L NaCl aggressive solution after immersion for 240 h at 35 °C

$C_{NaCl}$ (g/L)	Time /h	$R_s$ ( $\Omega \cdot \text{cm}^2$ )	$CPE$ ( $\Omega^{-1} \cdot \text{s}^{-n} \cdot \text{cm}^{-2}$ )	$n$	$R_{ct}$ ( $\Omega \cdot \text{cm}^2$ )
40	72	1.22	$9.86 \times 10^{-4}$	0.79	$2.29 \times 10^3$
	120	2.04	$1.09 \times 10^{-3}$	0.80	$1.82 \times 10^3$
	168	3.14	$1.34 \times 10^{-3}$	0.78	$9.17 \times 10^2$
	240	1.60	$1.90 \times 10^{-3}$	0.65	$8.13 \times 10^2$
60	72	0.62	$4.71 \times 10^{-4}$	0.66	$2.11 \times 10^3$
	120	1.36	$9.54 \times 10^{-4}$	0.75	$1.50 \times 10^3$
	168	2.66	$1.09 \times 10^{-3}$	0.81	$8.17 \times 10^2$
	240	1.59	$8.78 \times 10^{-4}$	0.84	$6.81 \times 10^2$
70	72	0.94	$1.36 \times 10^{-3}$	0.78	$1.13 \times 10^3$
	120	3.38	$1.10 \times 10^{-3}$	0.82	$1.00 \times 10^3$
	168	5.05	$1.21 \times 10^{-3}$	0.80	$8.72 \times 10^2$
	240	7.71	$1.23 \times 10^{-3}$	0.75	$6.57 \times 10^2$

### 3.2. Corrosion products after immersion testing

After immersion in NaCl solution for 240 hours, the surfaces of the FeCrNiTi soft magnetic alloy specimens were slightly corroded with a small amount of corrosion products, but some red corrosion product precipitates were observed in the immersion solution (Fig. 4a). After vacuum-filtration of the solution, the collected corrosion products were dried at 100 °C and then a black brown solid powder was obtained (Fig. 4b). The obtained products were tested by XRD (Fig. 4c). The XRD pattern indicates that the solid powder mainly consisted of NaCl and corrosion products including  $\text{Fe}(\text{OH})_3$ ,  $\text{FeOOH}$ , and  $\gamma\text{-Fe}_2\text{O}_3$ . The relatively loose corrosion products tended to fall off and precipitate in the NaCl aggressive solution with longer immersion time. In addition, the ferrous ions caused by anodic corrosion dissolution also diffused into the NaCl solution and were further oxidized by oxygen to form new iron oxides, hydroxides, and hydroxyl oxides. It is well known that chemical composition can significantly affect the magnetic behavior of magnetic materials [21]. After the FeCrNiTi specimens were corroded in NaCl solution, changes in the compositional structure were observed in the local area of the surface. In particular, the corrosion products are non-ferromagnetic phases, which can affect the magnetic properties.



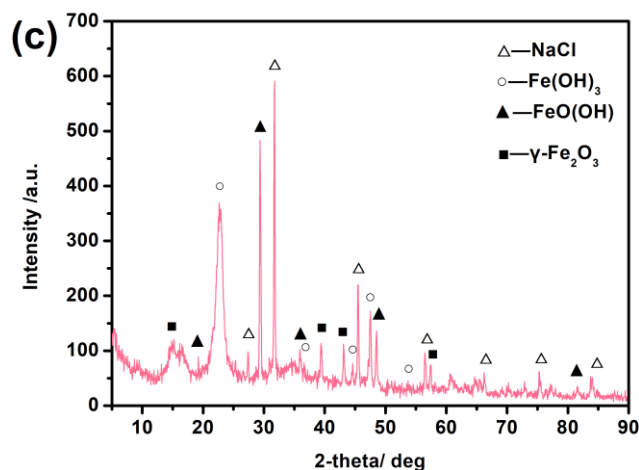


**Figure 4.** Appearance of tested specimens and NaCl solution (a), corrosion products powder (b), XRD pattern of corrosion products (c) of FeCrNiTi soft magnetic alloy specimens in 60 g/L NaCl aggressive solution after immersion for 240 h at 35 °C

### 3.3. Magnetic properties and corrosion morphology after salt spray testing

#### 3.3.1 Corrosion morphology

The corrosion morphology of FeCrNiTi soft magnetic alloys after different salt spray times (0, 24, 200 h) were analyzed, as shown in Fig. 6a-c. From the SEM images of corrosion morphology, it can be seen that some corrosion pits began to occur after the salt spray test, and the longer the salt spray time, the deeper the corrosion pits and the larger the corrosion area. After 200 h, even some of the deep pits continued to develop outward, finally connecting to each and causing more serious corrosion. In the process of salt spray corrosion, chloride ions play a major role. They have strong penetration ability and can easily penetrate the metal oxide layer into the metal interior and destroy the passive state of the metal. At the same time, chloride ions have very low hydration energy, which can be easily adsorbed on the metal surface to replace the oxygen in the oxide layer protecting the metal, so that the metal is damaged.

The corresponding EDS of the complete surface regions (Regions A, C, and E) with no obvious pitting corrosion after salt sprays of 0, 24, and 200 h are given in Fig. 6-f, respectively. The corresponding EDS of the complete surface regions (Regions B, D, and F) with pitting corrosion are shown in Fig. 6g-i, respectively. In all EDS maps of FeCrNiTi soft magnetic alloys, the main elements of Fe, Cr, Ti, etc. were detected. Typically for FeCrNiTi soft magnetic alloys, its high chromium content (~18%) can react easily with oxygen giving rise to an oxide layer on the surface. This passive layer mainly consists of hydrated chromium oxyhydroxide acting as a protective barrier against aggressive environments, thereby improving the corrosion resistance of the alloy [22,23]. Significantly, the content of Ti in the complete surface area regions (Regions A, C, and E) reached about 80 wt.%, which means that the surface was covered with a layer of Ti-rich film. In the corrosion pits (Regions B, D, and F), Fe and Cr accounted for about 90 wt.%, while Ti only accounted for 2 wt.%. The relationship between the distribution of Ti and the corrosion resistance of the alloy shows that the pitting corrosion caused by salt

spray testing occurred preferentially in the surface area with low Ti content, and the area covered with high Ti-containing surface film showed strong corrosion resistance, which means that the content and distribution of Ti on the surface of FeCrNiTi soft magnetic alloy had a significant effect on its corrosion resistance. The aforementioned sudden increase in corrosion current density in the potentiodynamic polarization test should be due to the rupture of this high Ti- and Cr-containing surface film. It is worth noting that the corrosion product film and the high Ti- and Cr-containing surface protective film may affect the magnetic properties of the FeCrNiTi alloy. As mentioned before in many cases, the effect of corrosion on the magnetic properties of magnetic material is explained by the presence of non-conductor and/or non-magnetic oxides on the oxidized surfaces [3].

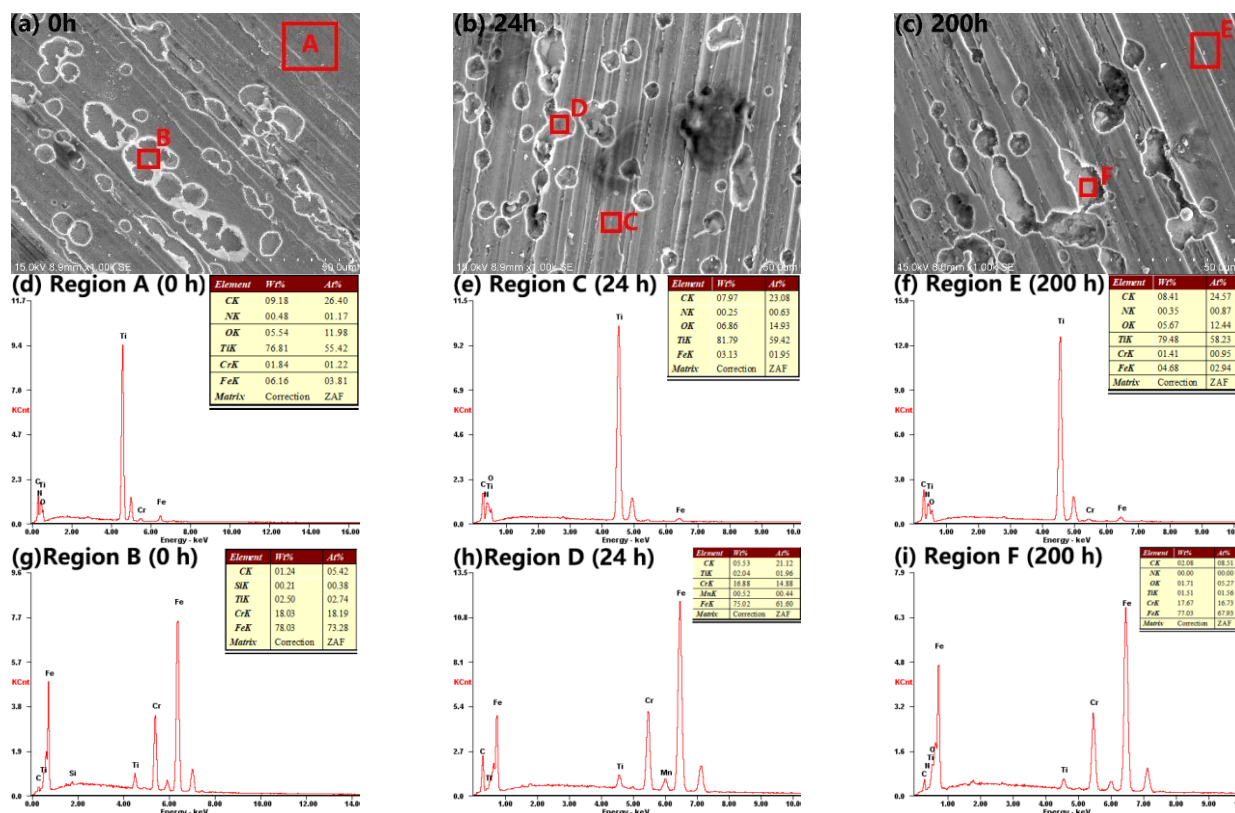


**Figure 6.** Corrosion morphology and EDS analysis of the FeCrNiTi soft magnetic alloy after different salt spray times (0 h, 24 h, 200 h)

### 3.3.2 Magnetic properties

The influence of different salt spray corrosion times (24, 48, 72 and 200 h) on the magnetic properties of soft magnetic alloy FeCrNiTi is shown in Fig. 5. It can be seen from Fig. 5 that the initial magnetic permeability ( $\mu_i$ ), maximum magnetic permeability ( $\mu_m$ ), and saturation magnetization ( $B_s$ ) decreased significantly, while the coercivity ( $H_c$ ), remanent magnetization ( $B_r$ ), and hysteresis loss ( $P_u$ ) increased with increasing salt spray corrosion time. The significant changes of these important properties indicate that the soft magnetic properties were degraded by the salt spray corrosion. The degradation of

the soft magnetic properties with increasing corrosion could be related to the corroded film formation [24,25]. Hayashi *et al.* [7] also found that magnetic properties change with corrosion because magnetic properties are strongly affected by the material surface quality, that is, the influence of corrosion on magnetic properties is a surface phenomenon [3].

The corrosion of metal materials by salt spray is mainly caused by the penetration of conductive salt solution into the metal to produce a electrochemical reaction, thereby forming a "low potential metal-electrolyte solution-high potential impurity" micro galvanic system, which generates electron transfer, and the metal as the anode dissolves to form a new compound, namely a corrosion product. The corrosion product film can cause a larger coercive field ( $H_c$ ) [10]. The specimen becomes more permeable with longer corrosion time. In addition, the hysteresis loss in the case of the sample with long-term corrosion is more than the case of the sample with short-term corrosion. It can be concluded that the pitting corrosion induced by chloride ions from salt spray and the presence of the corrosion product film on this magnetic material have significant influences on its magnetic behavior of the FeCrNiTi alloy. Corrosion not only changes the magnetic properties of magnetic materials, but also destroys the integrity of magnetic materials, thus affecting their actual use.

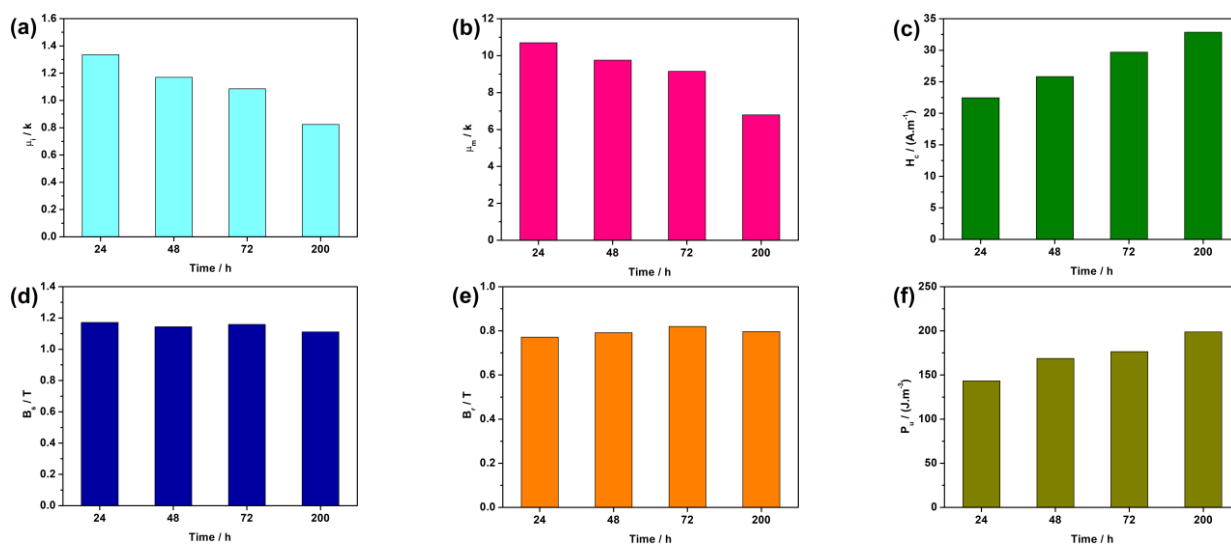


**Figure 5.** Effect of salt spray time on the magnetic properties of FeCrNiTi soft magnetic alloy specimens: (a) initial magnetic permeability ( $\mu_i$ ), (b) maximum magnetic permeability ( $\mu_m$ ), (c) coercivity ( $H_c$ ), saturation magnetization ( $B_s$ ), remanent magnetization ( $B_r$ ), and hysteresis loss ( $P_u$ )

As Sitek *et al.* [13] reported, the magnetic microstructure can be influenced by corrosion process. Corrosion can cause a change in direction of the net magnetic moment, intensity, and distribution of internal magnetic field [13]. Based on the results from salt spray testing and immersion testing, the main reasons for the degradation of magnetic properties of FeCrNiTi soft magnetic alloy include [26-28]: (1) iron oxide is precipitated in the matrix after corrosion and the precipitation of iron elements reduced the ferromagnetic elements in the matrix, resulting in decreased saturation magnetization. The iron oxide increased the magnetostrictive coefficient of the alloy, which can cause decreased magnetic

permeability; (2) After corrosion, some corrosion pits occurred on the substrate surface, which increased the internal stress on the substrate surface. The increase of internal stress can increase the magnetic anisotropy constant, thus reducing the magnetic permeability and degrading the soft magnetic properties.

#### 4. CONCLUSIONS

(1) The concentration of NaCl solution and the immersion time have an effect on the electrochemical corrosion behaviors of FeCrNiTi soft magnetic alloys. The corrosion can be accelerated by higher concentrations of NaCl solution and longer immersion times.

(2) The magnetic properties of FeCrNiTi soft magnetic alloys can be degraded by corrosion. With increasing corrosion time,  $\mu_i$ ,  $\mu_m$ , and  $B_s$  significantly decreased, while  $H_c$ ,  $B_r$ , and  $P_u$  increased. The degradation of the magnetic properties of FeCrNiTi soft magnetic alloys can be attributed to the formation of corrosion products, the precipitation of Fe elements from the matrix, and the internal stress induced by corrosion pits.

(3) The corrosion of FeCrNiTi soft magnetic alloys occurred preferentially in the surface area with low Ti content, and the area covered with high Ti-rich surface film showed strong corrosion resistance. The passive layer with certain content and distribution of Ti elements may act as a protective barrier against aggressive environments improving the corrosion resistance of the FeCrNiTi soft magnetic material.

#### ACKNOWLEDGEMENTS

This work was financially supported by the project of HDHDW5902020302.

#### References

1. Y. Yoshizawa, S. Oguma, and K. Yamauchi, *Journal of Applied Physics*, 64(1988)6044.
2. C. Liu, A. Inoue, F. L. Kong, E. Zanaeva and R. D. Shull, *Journal of Non-Crystalline Solids*, 554(2021)120606.
3. J. Garcia and A. Pierna, *Recent Patents on Materials Science*, 3(2010)13.
4. A. Gavrilovic, L. Rafailovic, W. Artner, J. Wosik and A.H. Whitehead, *Corrosion Science*, 53(2011)2400.
5. D. W. Rice, J. C. Suits and S. J. Lewis, *Journal of Applied Physics*, 47(1976)1158.
6. J. E. May, C. Souza, C. L. Morelli, N. A. Mariano and S. E. Kuri, *Journal of Alloys & Compounds*, 390(2005)106.
7. R. Hayashi, A. Yanagitani, Y. Aikawa and T. Sawada, US20080112841, 2008.
8. J. E. May, S. E. Kuri and P. A. P. Nascente, *Materials Science & Engineering A*, 428(2006)290.
9. N. A. Mariano, C. Souza, J. E. May and S. E. Kuri, *Materials Science & Engineering A*, 354(2003)1.
10. M. Ouadah, O. Touhami, R. Ibtouen, M. Khorchef and D. Allou, *Progress In Electromagnetics Research M*, 68(2018)79.
11. K. Peng, Y. Tang, L. Zhou, J. Tang, X. Feng and Y. Du, *Physica B Condensed Matter*, 366(2005)110.

12. D. Szewieczek and A. Baron, *Journal of Materials Processing Technology*, 164-165(2005)940.
13. J. Sitek, K. Sedlackova and M. Seberini, *Material Research in Atomic Scale by Moessbauer Spectroscopy*, 94(2003)159.
14. A. Baron, D. Szewieczek and G. Nawrat, *Electrochimica Acta*, 52(2007)5690.
15. I. Azoulay, C. Remazeilles and P. Refait, *Corrosion Science*, 58(2012)229.
16. S. Xu, J. Wang, N. Wang, T. Wang and Y. Wang, *Materials Today Communications*, 26(2021)101906.
17. V. N. Kytopoulos, A. Alzoumailis, C. Panagopoulos and C. Riga, *Procedia Structural Integrity*, 26 (2020)113-119.
18. H. Möller, E.T. Boshoff, H. Froneman, *The Journal of South African Institute of Mining and Metallurgy*, 106(2006) 585.
19. M. F. Pillis, G. A. Geribola, , G. Scheidt, E. G. D. Araújo, M. Oliveira, and R. A. Antunes, *Corrosion Science*, 102(2016)317.
20. S. Feliu, J. C. Galván and M. Morcillo, *Corrosion Science*, 30(1990)989.
21. M. Abshinova, *Procedia Engineering*, 76(2014)35.
22. M. F. López, M. L. Escudero, E. Vida, and A. R. Pierna, *Electrochem Acta*, 42(1997)659.
23. A. Pardo, E. Otero, M. C. Merino, M. D. López, M. Vázquez, and P. Agudoc, *Corrosion Science*, 43(2001)689.
24. A. Pardo, E. Otero, M. C. Merino, M. D. López, M. Vázquez, and P. Agudoc, *Corrosion Science*, 44 (2002) 1193.
25. C. A. C. Souza, M. F. de Oliveira, J. E. May, W. J. Botta, F. N. A. Mariano, S. E. Kuri, C. S. Kiminami, *Journal of Non-crystalline solids*, 273 (2000) 282.
26. C. A. C. Souza, D. V. Ribeiro and C. S. Kiminami, *Journal of Non-crystalline solids*, 442(2016)56.
27. C. A. C. Souza, J. E. May, I. A. Carlos, M. F. De Oliveira, S. E. Kuri, and C. S. Kiminami, *Journal of Non-Crystalline Solids*, 304(2002)210.
28. J. E. May, S. E. Kuri, and P. A. P. Nascente, *Materials Science & Engineering A*, 428(2006)290.